Plug-and-play, infrared, laser-mediated PCR in a microfluidic chip

**Nikita Pak · D. Curtis Saunders ·
Christopher R. Phaneuf · Craig R. Forest**

Abstract Microfluidic polymerase chain reaction (PCR) systems have set milestones for small volume (100 nL–5 μL), amplification speed (100–400 s), and on-chip integration of upstream and downstream sample handling including purification and electrophoretic separation functionality. In practice, the microfluidic chips in these systems require either insertion of thermocouples or calibration prior to every amplification. These factors can offset the speed advantages of microfluidic PCR and have likely hindered commercialization. We present an infrared, laser-mediated, PCR system that features a single calibration, accurate and repeatable precision alignment, and systematic thermal modeling and management for reproducible, open-loop control of PCR in 1 μL chambers of a polymer microfluidic chip. Total cycle time is less than 12 min: 1 min to fill and seal, 10 min to amplify, and 1 min to recover the sample. We describe the design, basis for its operation, and the precision engineering in the system and microfluidic chip. From a single calibration, we demonstrate PCR amplification of a 500 bp amplicon from λ-phage DNA in multiple consecutive trials on the same instrument as well as multiple identical instruments. This simple, relatively low-cost plug-and-play design is thus accessible to persons who may not be skilled in assembly and engineering.

Keywords PCR · Infrared · Microfluidic ·
High-throughput · Open-loop

Nikita Pak and D. Curtis Saunders contributed equally to this work.

N. Pak (✉) · D. C. Saunders · C. R. Phaneuf · C. R. Forest
George W. Woodruff School of Mechanical Engineering,
Georgia Institute of Technology,
Room 2103, 315 Ferst Drive,
Atlanta, GA, USA
e-mail: nikpak@gatech.edu

1 Introduction

Since its genesis in 1983 by Kary Mullis(Mullis and Faloona 1987), polymerase chain reaction (PCR) has become the standard technique for genetic diagnostics. By thermally cycling a biochemical cocktail and exponentially amplifying a specific region of RNA or DNA from as little as a single copy, PCR allows highly specific and sensitive detection of target sequences or in the case of "consensus-degenerate" PCR, a broad range of known and evolutionarily related sequences(Rose et al. 2003).

The speed and fidelity of PCR is determined by sample quality, assay design, and the means and precision of thermocycling. Since typical scenarios involve samples of unknown quality and fixed protocols, the thermocycling is critical. Most commercial thermocyclers use indirect conductive heating and are consequently slow (e.g., 3°C/s), have temperature inaccuracy and well-to-well variation(Kim et al. 2008; Yang et al. 2005), and require large sample volumes (e.g., 25 μL). Alternatives include the Roche Lightcycler(Wittwer et al. 1997) and Qiagen Rotor Gene Q that use convective heating and fluorescence detection for real-time PCR with volumes as low as several microliters. Though effective, their cost and complexity limit scalability, speed, compatibility with field deployment, and volume reduction. Most micro-scale PCR devices use thermally conductive silicon or glass microchips paired with thermoelectric heating(Khandurina et al. 2000; Matsubara et al. 2005; Nagai et al. 2001; Slyadnev et al. 2008), embedded resistive heaters(Liao et al. 2005; Lien et al. 2007; Liu et al. 2007; Minqiang et al. 2003; Neuzil et al. 2006; Northrup et al. 1998; Wang et al. 2006; Woolley et al. 1996; Xiang et al. 2005; Zou et al. 2003), or convection-based rotary platforms (Wittwer et al. 1997; Focke et al. 2010; Wheeler et al. 2004; Wittwer et al. 1990) to offer smaller reagent volumes and

faster cycling at the risk of costly fabrication and cross-contamination after multiple runs.

In contrast, direct heating via infrared radiation, pioneered by Dr. James Landers using a tungsten filament lamp(Easley et al. 2006; Hühmer and Landers 2000; Oda et al. 1998) and closed-loop feedback through a thermocouple, enables rapid microliter volume thermocycling in simple, inexpensive, disposable microchips. Others have performed infrared, laser-mediated, microfluidic PCR in droplets in an oil bath after fluorescence calibration(Slyandev et al. 2001; Kim et al. 2009; Terazono et al. 2008). They were able to achieve very impressive rapid (200 s), small volume (15 pL), real-time PCR results, but the system requires a precisely aligned microscope and the small, suspended droplets cannot be easily recovered for post-processing, making this instrument less practical for commercialization. Previous reports of calibration methods for infrared PCR have been limited by emissivity measurements with a pyrometer(Hühmer and Landers 2000) in which accuracy is hindered by alignment and spurious reflection, or required microscopy. Ultimately, commercial implementation and the speed advantages of infrared PCR in microfluidic chips have been hindered by at least one of the following requirements for every amplification run: (1) thermocouple insertion time and complexity, (2) optical alignment with microscopic (i.e. sub mm) accuracy and repeatability, or (3) calibration.

We have designed, manufactured, and tested an infrared radiative thermocycler and associated microfluidic chip that retains the advantages of infrared PCR systems (e.g., speed, low volume, low power consumption, low cost, compact form) while eliminating the need for thermocouple insertion and repeated active alignment and calibration. Open-loop temperature control from a *single* calibration run is used for *multiple* consecutive amplifications on *multiple* identical instruments. This temperature control is made possible by passive, precision-engineered alignment fixtures, accurate and repeatable polymer microchip design and fabrication methods, and systematic thermal management strategies. We describe the instrument and chip design, fabrication, and performance. We demonstrate its functionality with reproducible sub-10 min PCR amplification of a 500 bp amplicon from λ-phage.

2 Design overview

The system, shown in Fig. 1, consists of a 1450 nm infrared laser diode with heat sink and fan, collimating lens with x-y stage, and microchip holder. As we have shown in previous work(Phaneuf et al. 2011), this wavelength for infrared PCR is advantageous because it affords two orders of magnitude difference in absorption between the aqueous PCR solution and the surrounding polymer chip; an ideal environment for rapid (e.g. 60°C/s) cycling while retaining thermal isolation between adjacent chambers within a chip. The heat sink and fan keep the laser diode temperature and corresponding power output constant. The laser diode optical output power required is only 580 mW; the necessary electrical input power of 5 W is an order of magnitude less than all commercial thermocyclers and most research devices and thus facilitates portable and compact designs.

The collimating lens and x-y stage are used to align the laser to a reaction chamber on the chip by burning a hole in a piece of toner paper (not shown) attached to the chip. The x-y stage is adjusted until the toner paper hole and microchip reaction chamber are directly aligned. The microfluidic chip holder is a single poly (methyl methacrylate) (PMMA) part, as seen in Fig. 2 (a), consisting of a leaf spring and three points for full kinematic constraint in the x-y plane. The entire assembly rests on a standard 30 mm cage system. Translation of the optical assembly on this rod system allows microfluidic chip

Fig. 1 (**a**) Exploded view diagram of laser thermocycling system showing the laser source subsystem (*top*), collimation subsystem (*middle*), and microchip subsystem (*bottom*). *Dashed arrows* represent components that are embedded and not easily visible in the photograph. (**b**) Photograph of laser system, where the *dotted line arrow* represents the movement of the laser and lens assembly for loading the microchips into the chip holder
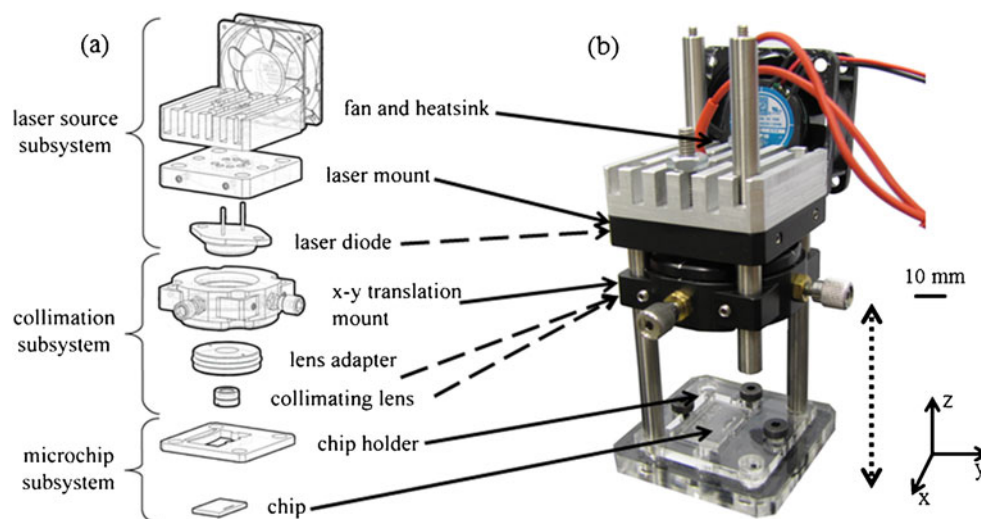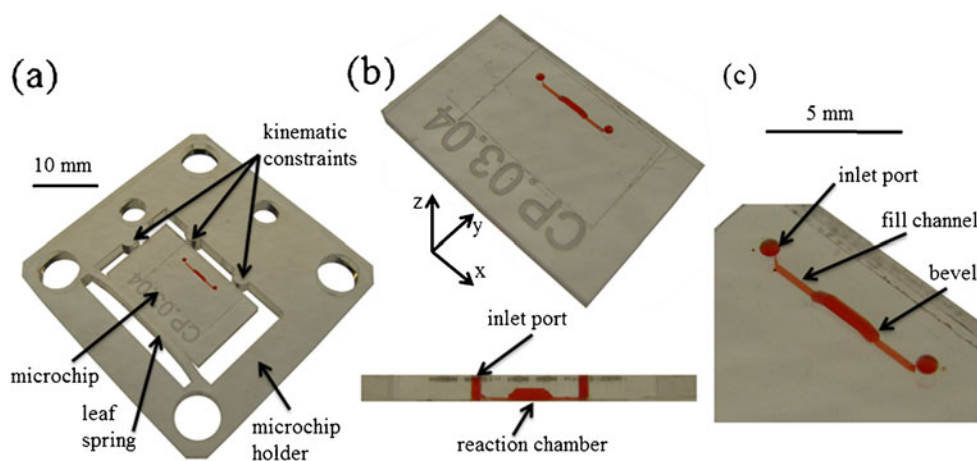
Fig. 2 (**a**) Photograph of poly (methyl methacrylate) (PMMA) chip holder showing kinematic constraints, leaf spring, and microchip, (**b**) isometric view and side profile of PMMA microchip, (**c**) and close up of reaction chamber showing inlet port, fill channel, and beveled reaction chamber

insertion and removal. Associated electronics not shown in Fig. 1 are the laser driver, power supply, and data acquisition board. These are sized similarly such that the total system volume is on the order of 200 mm^3.

Using Labview, we implemented software for analog open-loop laser driving voltage control. The inputs (voltage, time) are run from a text file. To operate the system, the chip is filled with the requisite PCR solution, positioned, the laser assembly is lowered onto the chip, and the Labview program is initiated. The total amount of time for filling, sealing, and subsequently recovering the sample from the chips after the run with a pipettor is less than 1 min.

3 Polymer chip design and fabrication

The microchips, seen in Fig. 2(b) and (c) feature inlet ports on both sides of the reaction chamber that allow standard pipette tips to easily fill the chamber. Narrow fill channels lead to the reaction chamber to minimize diffusion, and the beveled chamber geometry helps to ensure complete filling and easier thermocouple insertion when required for calibration. Microchips were fabricated from PMMA at a rate of two chips per minute, using a 3-axis vertical milling center (Haas, OM-1A) capable of accurate positioning within 10 μm and repeatability of 6 μm. The spindle operates at speeds up to 30,000 rpm, enabling the use of miniature end mills (Harvey Tool) and drill bits (Drill Bit City) with sub-millimeter diameters. These tools are zeroed to the polymer workpiece by detecting electrical conductivity between the tool tip and the base of a custom aluminum fixture(Sodemann and Mayor 2009) that was milled and used to align and rigidly hold the polymer workpiece, since small part deflections can easily damage the fragile tooling. A corner relief was pocketed into the fixture along with features for interfacing with a standard vise to allow repeatable positioning. Strap clamps were laser cut from 3.175 mm acrylic, which

was chosen to avoid marring the surface of the workpiece. These were configured in a third-class lever arrangement and the screws were hand-tightened to provide clamping force sufficient to overcome cutting forces. Toolpaths were manually written in G-code to achieve the relatively simple designs but can also be programmed using computer-aided manufacturing (CAM) software for complex geometries. During the milling process, compressed air was used for clearing chips and preventing burr formation. Following milling, microchips were ethanol rinsed, dried with pure nitrogen, and the bottoms were sealed by a simple thermal bonding process with a 100 μm polymer film on a hot plate at 155°C, 30 min, and 100 psi for a 20 mm×10 mm microchip. The top of the chip is sealed after filling with an optically transparent and biologically compatible adhesive film (Excel Scientific, ThermalSeal RT). Microchips have been used repeatedly without polymer delamination or damage, yet the adhesive film is easily peeled away manually.

This micro-milling process has been invaluable during the prototyping phase of this work. Altering a design and making a new batch of microchips can be easily accomplished in less than 1 day. Materials such as PMMA, polycarbonate, and a biocompatible grade of cyclic olefin copolymer (COC) have all been successfully used for a substrate. PMMA was chosen because it is most quickly machinable, while retaining excellent optical, thermal, and biocompatible properties(Lee et al. 2004). Another advantage is the three-dimensional geometries attainable with micro-milling in order to create path lengths amenable to maximum absorption as well as control of the surface-area-to-volume ratio for optimum heat transfer characteristics and minimal adsorption of biological reagents to the interior microchip surfaces.

4 Thermal modeling

To better understand how an aqueous solution within a polymer chamber is heated by radiation, a computational

model (Matlab, Mathworks, Natick, MA) was created that predicts the radiation absorption as a function of distance through the aqueous solution, or pathlength. We have described in detail this approach earlier(Phaneuf et al. 2011), and so summarize it here only briefly. First, the spectral irradiance of the source is scaled by integrating over its full spectrum and equating this with the measured total power output, yielding the spectral power distribution, $P_0(\lambda)$. This is then attenuated uniformly by accounting for losses due to reflection at the air-polymer interface. Finally, the power absorbed by the aqueous solution as a function of wavelength, $P_{ABS}(\lambda)$, is calculated using the Beer-Lambert Law as $P_{ABS}(\lambda)=P_0(\lambda)(1-10^{-\alpha(\lambda)l})$, where $\alpha(\lambda)$ is the wavelength dependent absorption coefficient of PMMA and l is the pathlength. Integration with respect to wavelength yields the total power absorbed as a function of distance. Applying this model to our microfluidic chip, aqueous solution, and laser resulted in 90% power absorption after 0.5 mm of radiation propagation through the solution (z-axis direction).

To compute the temperatures in the aqueous solution resulting from this radiation absorption, we implemented a finite element model (COMSOL, Stockholm, Sweden). We were most concerned with the temperature variation along the z-axis through the chamber in the direction of radiation propagation along the chamber centerline (x=y=0), where the temperature is highest in the x-y plane. To implement the model, we divided the chamber into equal volumetric sections spanning the x-y cross-section, and assigned heat generation power to each of them based on the pathlength-dependent absorption model described above. For our design, we selected a total laser power output of 580 mW, absorbed by five volumetric sections in the direction of radiation propagation absorption; each section 150 µm thick. Respectively, the radiation absorbed and corresponding centerline temperature of each section was 60.6% yielding 93.4°C, 21.1% yielding 90.2°C, 7.35% yielding 83.4°C, 2.56% yielding 77.7°C, and 0.89% yielding 73.1°C. Thus the total predicted temperature variation through the 750 µm deep chamber along the z-axis is 20.3°C. We experimentally measured a temperature gradient of 8°C with a thermocouple (T240-C, Physitemp, Clifton, NJ), and attribute the difference to the thermocouple's physical size of 130 µm in diameter and its location approximately 100 µm from the bottom of the chamber. These thermal modeling results proved useful in our calibration efforts.

5 Calibration

In order to utilize open-loop control, a calibration curve relating laser driving voltage to aqueous solution temperature is necessary. The calibration curve for our system is

seen in Fig. 3. The thermocouple used for calibration is heated directly by the laser, so calibration requires measuring and compensating for this bias error as follows. First, it was known that the threshold voltage for the laser to turn on was 0.25 V. At this driving voltage the bias is zero and the thermocouple reads a temperature of 33°C, identical to the chamber temperature. Next, the driving voltage was increased as the reaction chamber was observed with a microscope. Boiling, as indicated by the rapid formation and expansion of bubbles in the chamber, occurred at 1.1 V and corresponds to 100°C at atmospheric pressure.

With the thermocouple centered and positioned at the bottom of the chamber, the measured bias increases from 0°C at 0.25 V to around 8°C at 1.1 V. The variables affecting this bias include thermocouple placement repeatability, bubble formation, and direction the thermocouple tip is bent. A special calibration microchip was manufactured with the thermocouple bonded to the bottom layer. This prevents many of these variations between runs because the thermocouple tip is in the same position every time. Also, since our thermal modeling predicted that 90% of the radiation is absorbed in the first 0.5 mm of the aqueous solution, confounding effects of radiation heating of the thermocouple directly were minimized with the thermocouple located at the bottom of the chamber. A polynomial was fit to the bias corrected temperature measurements, resulting in the calibration curve shown in Fig. 3.

Once this curve is created, it can be used to find the three voltages corresponding to the denaturing, annealing, and extension temperatures of the particular amplification to be performed. While these three voltages are all that is required, slow temperature ramping under such a simple control scheme would necessitate hours for one amplification run. Therefore, to expedite heating and cooling, we applied the maximum driving voltage and then a holding voltage corresponding to the denaturing temperature. Similarly for cooling, a zero voltage
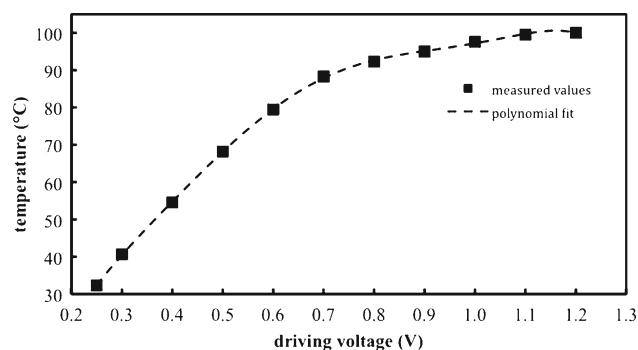

Fig. 3 Calibration curve relating laser driving voltage and aqueous solution steady state temperature used for open-loop temperature control

duration precedes the annealing voltage. A typical three temperature PCR cycling program thus requires five distinct driving voltages: maximum power to ramp up to denaturing, a denaturing holding voltage, zero voltage to cool to annealing, an annealing holding voltage, and an extension holding voltage. If there is a significant temperature difference between the annealing and extension temperatures, a sixth full power ramping voltage can be implemented between those two holds. The heating and cooling times are measured and set to minimize under- and over-shoot. The resulting temperature profile and driving voltage can be seen in Fig. 4. Desired times and temperatures were 4 s at 90°C for denaturing, 5 s at 68°C for annealing, and 5 s at 72°C for extension.

6 Mechanical and thermal repeatability

In order for open-loop control to work consistently, thermal and mechanical repeatability are paramount. As described previously, the x-y stage to position the collimating lens is only adjusted once. However, the laser beam alignment is periodically checked to ensure identical heating by burning a piece of toner paper as mentioned previously. Although it is rarely out of alignment, this test takes less than 1 min to perform and ensures consistency.

To measure the repeatability of the chip alignment in the holder, we mounted the system on an inverted microscope (Nikon, TE2000-E) to image the chip location during repeated placement. Of the three principal system axes, shown in Fig. 1, the x-axis error is insensitive because this axis is parallel to the reaction chamber's length and deviations less than 1 mm do not cause significant temperature differences.

For the y-axis alignment repeatability measurement, we placed and imaged the chip five times. The standard deviation measured was $\sigma_y=5.31$ μm, causing no measurable temperature difference with thermocouple inserted into the chamber and laser heating. This same test is repeated each time a new batch of chips is made to make sure they are within specification.

For the z-axis repeatability measurement, or direction normal to the chip surface, we repeatedly focused the microscope on either a stationary chip or a successively removed and replaced chip. From the stationary chip, we ascertained from five measurements that the standard deviation of the focusing error was 9.9 μm. From five measurements with the replaced chip, which includes this focusing error, the standard deviation of the position measured was $\sigma_z=16.4$ μm. To determine if this error was problematic, we measured the temperature variation corresponding to z-axis translation between the laser and chip. For a 1,000 μm displacement, more than the 750 μm chamber height, a temperature variation of only 0.5°C was measured, so the σ_z measured was deemed acceptable.

To measure the *combined* repeatability of the chip placement, laser z-axis translation to allow chip placement, laser power output, and thermocouple placement for calibration, we successively removed, replaced, and heated a water-filled chip and its thermocouple. Five consecutive temperature measurements showed a standard deviation of 0.1°C, well within tolerances for PCR from conventional instruments. We note that the primary cause of the difference in temperatures between the trials is the result of variations in thermocouple placement, which is not used during PCR.

Fig. 4 Experimental temperatures obtained from calibration and corresponding laser open-loop control voltages for PCR of 500 bp DNA amplicon in 9:58 in a 1 μL chamber within a polymer microfluidic chip
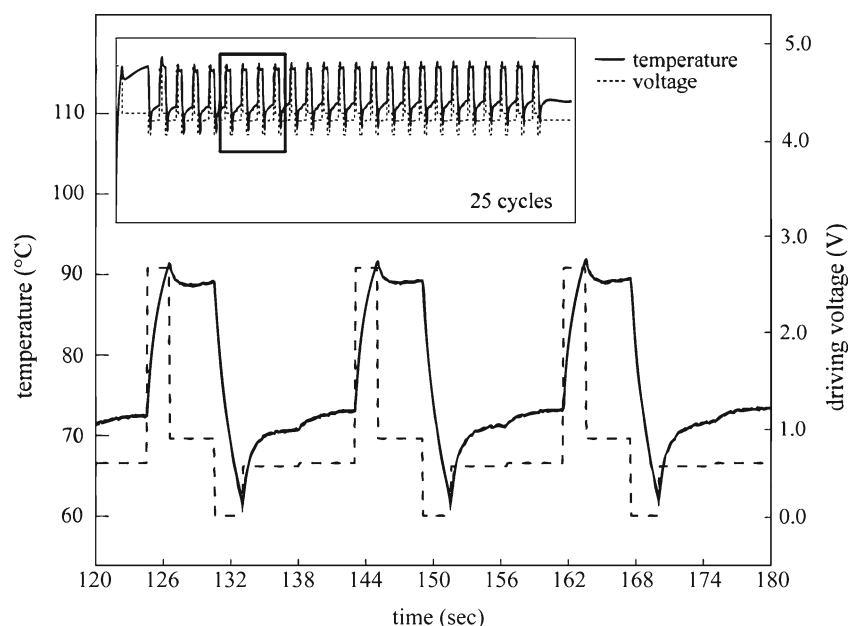
7 PCR amplification of λ-phage DNA

As a means to verify our system and method, an amplification of λ-phage DNA was performed on both our laser-based system and a conventional Peltier-based thermocycler (Biorad, MJ Mini). The reaction solution was prepared in quantities of 5 μL volumes according to the following protocol: 0.5 μL 10X PCR buffer, 0.8 μL $MgCL_2$ (25 mM), 0.1 μL dNTP mixture (10 mM), 0.1 μL forward and reverse primers (20 μM), 1.2 μL BSA (1 mg/mL), 1.0 μL DNA (45.8 μg/mL), 1.2 μL water, and 0.1 μL Taq polymerase. BSA has previously been shown to aid microchip PCR(Zhang et al. 2006). The primer sequences used were 5′-GATGAGTTCGTGTTCGTACAACTGG-3′ for the forward primer and 5′-GGTTATCGAAATCAGCCAC AGCGCC-3′ for the reverse primer. Our microchips were loaded with about 1,400 nL, of which approximately 820 nL was located within the chamber. After running the 25-cycle program as seen in Fig. 4, we evaluated results with microchannel electrophoresis separation (Agilent, Bioanalyzer). Successful amplification with excellent signal to noise ratio (>200:1), for a typical trial are shown in Fig. 5.

This amplification was performed in less than 10 min, with a total setup, recovery, and run time of less than 12 min. Five identical runs were performed in series with the same outcome, demonstrating the repeatable DNA amplification achievable with our device.

It should be noted that the calibration curve is unique to the microfluidic chip design and laser used. However, these variables are easy to maintain, and we have used the same calibration curve on two identical laser thermocycler systems that we have constructed to obtain DNA amplification with no adjustments. If a new microchip design or a different laser is used, the calibration curve can be created in approximately 3 h. This process has an initial time investment, but greatly reduces the amount of time needed for each machine run.

8 Conclusions

The operation of this plug-and-play infrared-mediated PCR system has the advantages previously seen in microfluidic PCR systems, but operates more like a conventional PCR instrument in that the user simply loads and places the chip or well plate into the instrument, and removes it following amplification for sample post-processing. From a precision optical and mechanical design, thermal modeling, control, and calibration we were able to show repeatable DNA amplification in less than 10 min on a microchip of a volume of less than 1 μL in a system that requires little user interface and has a total run time of less than 12 min. This approach is not restricted to low-cost microfluidic volumes (e.g., 1 μL), thus increasing utility. We have previously cycled 10 μL with our prototype using standard PCR tubes in place of the microchip. With higher laser power and beam size control, we can cycle these larger volumes faster than conventional instruments while maintaining the advantages of open-loop and potentially multiplexed temperature control. In the future, these advantages will allow us to easily modify our device for performing real time PCR using the microscope previously mentioned. Also, scaling up to multiple reaction chambers on one microchip can now be achieved without having to simultaneously scale up the temperature measurement system. If the radiation is optically manipulated, there is potential for unprecedented scalability and independent temperature control of multiple PCR chambers on a single microchip. The open-loop control scheme allows this to be done in a similar total time as the one reaction chamber chip.

Fig. 5 Electropherogram of 500 base pair lambda DNA amplification performed in less than 10 min on a 1 μL polymer microchip. This was repeated five times with identical results
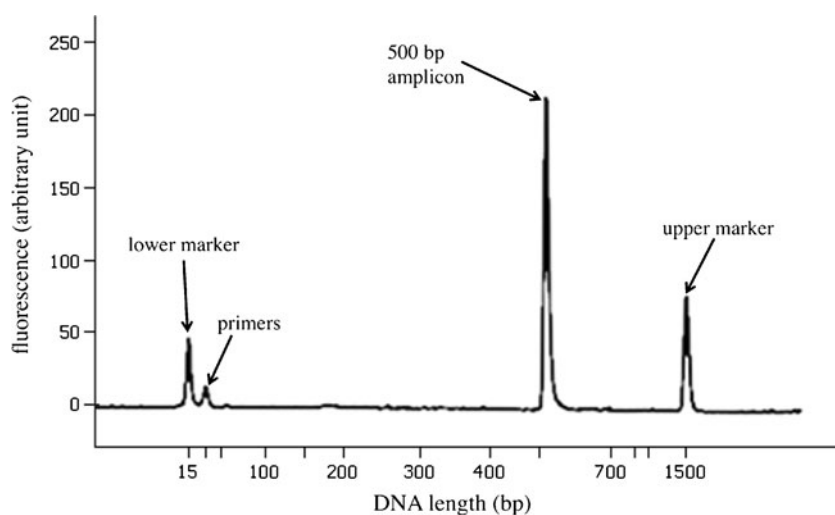
References

K.B. Mullis, F.A. Faloona, *Specific synthesis of DNA in vitro via a polymerase-catalyzed chain reaction* (ETATS-UNIS: Elsevier, San Diego, 1987)

T.M. Rose, J.G. Henikoff, S. Henikoff, CODEHOP (COnsensus-DEgenerate Hybrid Oligonucleotide Primer) PCR primer design. Nucleic Acids Res. **31**, 3763–3766 (2003)

Y.H. Kim, I. Yang, Y.S. Bae, S.R. Park, Performance evaluation of thermal cyclers for PCR in a rapid cycling condition. Biotechniques **44**, 495–505 (2008)

I. Yang, Y.H. Kim, J.Y. Byun, S.R. Park, Use of multiplex polymerase chain reactions to indicate the accuracy of the annealing temperature of thermal cycling. Anal. Biochem. **338**(2), 192–200 (2005)

C.T. Wittwer, K.M. Ririe, R.V. Andrew, D.A. David, R.A. Gundry, U.J. Balis, The LightCycler(TM) a microvolume multisample fluorimeter with rapid temperature control. Biotechniques **22**(1), 176–181 (1997)

J. Khandurina, T.E. McKnight, S.C. Jacobson, L.C. Waters, R.S. Foote, J.M. Ramsey, Integrated system for rapid PCR-based DNA analysis in microfluidic devices. Anal. Chem. **72**(13), 2995–3000 (2000)

Y. Matsubara, K. Kerman, M. Kobayashi, S. Yamamura, Y. Morita, E. Tamiya, Microchamber array based DNA quantification and specific sequence detection from a single copy via PCR in nanoliter volumes. Biosens. Bioelectron. **20**(8), 1482–1490 (2005)

H. Nagai, Y. Murakami, K. Yokoyama, E. Tamiya, High-throughput PCR in silicon based microchamber array. Biosens. Bioelectron. **16**(9–12), 1015–1019 (2001)

M. Slyadnev, M. Lavrova, M. Erkin, V. Kazakov, A. Ganeev, Development of a multireactor microfluidic system for the determination of DNA using real-time polymerase chain reaction. J. Anal. Chem. **63**(2), 192–198 (2008)

C.-S. Liao, G.-B. Lee, H.-S. Liu, T.-M. Hsieh, C.-H. Luo, Miniature RT-PCR system for diagnosis of RNAbased viruses. Nucleic Acids Res. **33**(18), e156 (2005)

K.-Y. Lien, W.-C. Lee, H.-Y. Lei, G.-B. Lee, Integrated reverse transcription polymerase chain reaction systems for virus detection. Biosens. Bioelectron. **22**(8), 1739–1748 (2007)

P. Liu, T.S. Seo, N. Beyor, K.-J. Shin, J.R. Scherer, R.A. Mathies, Integrated portable polymerase chain reaction-capillary electrophoresis microsystem for rapid forensic short tandem repeat typing. Anal. Chem. **79**(5), 1881–1889 (2007)

B. Minqiang et al., Design and theoretical evaluation of a novel microfluidic device to be used for PCR. J. Micromech. Microeng. **13**(4), S125 (2003)

P. Neuzil, C. Zhang, J. Pipper, S. Oh, L. Zhuo, Ultra fast miniaturized real-time PCR: 40 cycles in less than six minutes. Nucleic Acids Res. **34**(11), e77 (2006)

M.A. Northrup, B. Benett, D. Hadley, P. Landre, S. Lehew, J. Richards et al., A miniature analytical instrument for nucleic acids based on micromachined silicon reaction chambers. Anal. Chem. **70**(5), 918–922 (1998)

Z. Wang, A. Sekulovic, J.P. Kutter, D.D. Bang, A. Wolff, Towards a portable microchip system with integrated thermal control and polymer waveguides for real-time PCR. Electrophoresis **27**(24), 5051–5058 (2006)

A.T. Woolley, D. Hadley, P. Landre, A.J. de Mello, R.A. Mathies, M.A. Northrup, Functional integration of PCR amplification and capillary electrophoresis in a microfabricated DNA analysis device. Anal. Chem. **68**(23), 4081–4086 (1996)

Q. Xiang, B. Xu, R. Fu, D. Li, Real time PCR on disposable PDMS chip with a miniaturized thermal cycler. Biomed. Microdevice **7**(4), 273–279 (2005)

Q.B. Zou, U. Sridhar, Y. Chen, J. Singh, Miniaturized, independently controllable multichamber thermal cycler. IEEE Sensors J. **3**(6), 774–780 (2003)

M. Focke, F. Stumpf, G. Roth, R. Zengerle, F. von Stetten, Centrifugal microfluidic system for primary amplification and secondary real-time PCR. Lab Chip (2010)

E.K. Wheeler, W. Benett, P. Stratton, J. Richards, A. Chen, A. Christian et al., Convectively driven polymerase chain reaction thermal cycler. Anal. Chem. **76**(14), 4011–4016 (2004)

C.T. Wittwer, G.C. Fillmore, D.J. Garling, Minimizing the time required for DNA amplification by efficient heat transfer to small samples. Anal. Biochem. **186**(2), 328–331 (1990)

C.J. Easley, J.M. Karlinsey, J.M. Bienvenue, L.A. Legendre, M.G. Roper, S.H. Feldman, J.P. Landers, A fully integrated microfluidic genetic analysis system with sample-in-answer-out capability. Proc. Natl. Acad. Sci. **103**(51), 19272–19277 (2006)

A.F.R. Hühmer, J.P. Landers, Noncontact infrared-mediated thermocycling for effective polymerase chain reaction amplification of DNA in nanoliter volumes. Anal. Chem. **72**(21), 5507–5512 (2000)

R.P. Oda, M.A. Strausbauch, A.F.R. Huhmer, N. Borson, S.R. Jurrens, J. Craighead et al., Infrared mediated thermocycling for ultrafast polymerase chain reaction amplification of DNA. Anal. Chem. **70**(20), 4361–4368 (1998)

M. Slyandev, Y. Tanaka, M. Tokeshi, T. Kitamori, Photothermal temperature control of a chemical reaction on a microchip using an infrared diode laser. Anal. Chem. **73**, 4037–4044 (2001)

H. Kim, S. Vishniakou, G.W. Faris, Petri dish PCR: laser-heated reactions in nanoliter droplet arrays. Lab Chip **9**(9), 1230–1235 (2009)

H. Terazono, A. Hattori, H. Takei, K. Takeda, K. Yasuda, Development of 1480 nm photothermal highspeed real-time polymerase chain reaction system for rapid nucleotide recognition. Jpn. J. Appl. Phys. **47**, 5212 (2008)

C.R. Phaneuf, N. Pak, C.R. Forest, Modeling radiative heating of liquids in microchip reaction chambers. Sens. Actuators, A **167**, 531–536 (2011)

A.A. Sodemann, J.R. Mayor, Parametric investigation of precision in tool-workpiece conductivity touch-off method in micromilling. Trans. N. Am. Manuf. Res. Inst. SME **37**, 565–572 (2009)

D.S. Lee, S.H. Park, H. Yang, K.H. Chung, T.H. Yoon, S.J. Kim, K. Kim, Y.T. Kim, Bulk-micromachined submicroliter-volume PCR chip with very rapid thermal response and low power consumption. Lab Chip **4**, 401–407 (2004)

C. Zhang, J. Xu, W. Ma, W. Zheng, PCR microfluidic devices for DNA amplification. Biotechnol. Adv. **24**(3), 243–284 (2006)